THE JACOBIAN DERIVATIVE METHOD FOR THREE-DIMENSIONAL FRACTURE MECHANICS

E. J. BARBERO

Department of Mechanical and Aerospace Engineering, West Virginia University, Morgantown, WV, U.S.A.

AND

J. N. REDDY

Department of Engineering Science and Mechanics, Virginia Polytechnic Institute and State University, Blacksburg, VA, U.S.A.

SUMMARY

This paper presents a new algorithm to compute the distribution of the strain energy release rate along the crack front for three-dimensional cracks (e.g surface cracks). The algorithm is economical and accurate. The algorithm is illustrated via two-dimensional and three-dimensional examples including a surface crack in a cylinder under internal pressure and side-grooved compact-test specimens. It is shown, via specific examples, that only a single, self-similar virtual crack extension is necessary to accurately compute the strain-energy release-rate distribution along the crackfront.

INTRODUCTION

The finite-element method is well established as a tool for determination of stress intensity factors in fracture mechanics. Isoparametric elements are among the most frequently used elements due to their ability to model the geometry of complex domains. The quarter-point element[1,2] became very popular in linear elastic fracture mechanics (LEFM) because it can accurately represent the singularities in those problems. Its use has been extended to other problems as well.[3]

Two main areas have received attention in fracture mechanics analyses: (i) to model accurately the singular behaviour near the crack front; (ii) to compute the stress intensity factor from the solution to the finite-element model of the problem. The present study deals with the second problem, with emphasis on the use of isoparametric elements. The method presented here has its origins in the virtual crack extension method of Hellen[4] and the stiffness derivative method of Parks.[5] But in contrast to the VCEM, the Jacobian derivative method presented herein does not require an arbitrary choice of a 'virtual' extension that in the VCEM becomes an 'actual' extension. We take advantage of the isoparametric formulation to compute the strain energy release rates directly from the displacement field.

The Jacobian derivative method is a true post-processor algorithm. In this method the stress intensity factors are computed from an independently obtained displacement solution. Therefore, the displacement solution can be obtained with a program without any fracture mechanics capability, although adequate representation of the singular behaviour near the crack front is necessary. The displacement field may even be obtained by experimental techniques. Furthermore, the proposed technique does not require computation of stresses,

thus reducing computational cost and increasing accuracy. The Jacobian derivative method also provides the distribution of the strain energy release rate along the crack front, $G = G(s)$, without any two-dimensional hypothesis (here s denotes a curvilinear co-ordinate along the crack front).

The present study is motivated by delamination-type problems in composite laminates. These problems exhibit planar growth – that is, the crack grows in its original plane. However, the shape of the crack may vary with time. For example, an initially elliptic crack usually grows with variable aspect ratio. Therefore we cannot in general assume self-similar crack growth. The algorithm presented is simple, inexpensive, reliable and robust. The following literature forms a background for the present study.

Numerous methods for the calculation of stress-intensity factors have appeared over the years. The direct methods are those in which the stress-intensity factors are computed as a part of the solution. The direct methods require special elements that incorporate the crack tip singularity.[6] The indirect methods are those in which the stress-intensity factors are computed from displacements or stresses that are obtained independently. The more popular indirect methods are: extrapolation of displacements or stresses around the crack tip[7] and the nodal-force method.[8,9] Integral methods like the J-integral method,[10] the modified crack closure integral,[11,12] and the virtual crack extension method[4,5] are also used. The indirect methods can be used with conventional elements or with special elements that incorporate the singularity at the crack front.

The virtual crack extension method (VCEM) is appealing because it does not require computation of stresses, and therefore is inexpensive and accurate. However, the VCEM requires two computations for two slightly different configurations. Improved versions of the VCEM[4] or the stiffness derivative method[5] eliminate the second run but require the specification of a 'virtual' crack extension (VCE), a small quantity that must be chosen arbitrarily. Rounding errors may appear if the VCE is too small, and badly distorted elements may result if the VCE is too large.[4]

The virtual crack extension method postulates that the strain energy release rate can be computed as

$$G(s) = \frac{\partial U}{\partial a} \qquad (1)$$

where U is the strain energy and a is the representative crack length. In the actual implementation of VCE, however, one approximates equation (1) by the quotient $\Delta U / \Delta a$; in the limit $\Delta a \to 0$ gives the desired value of G.

The Jacobian derivative method proposed here computes $G(s)$ according to equation (1) exactly. The method does not require the approximation of the derivative, and therefore the choice of the magnitude of the 'virtual' crack extension does not arise. The concept has been already applied in other fields.[13] Similar but different methods have been developed.[14-17] The basic idea of the method can be summarized as follows. In the isoparametric formulation the geometry and the solutions are approximated with the same interpolation (or finite elements). Therefore, the total potential energy depends both on the displacements and on the nodal co-ordinates that ultimately represent the shape of the domain. Once the displacements have been found for a fixed configuration, the potential energy depends only on the nodal co-ordinates of the boundary. Consequently, we can compute the strain energy release rate due to a virtual crack extension simply by differentiating with respect to the nodal co-ordinates on the crack front. The nodal co-ordinates can be treated as variables in the isoparametric formulation of the problem. In the following Section we formally develop this idea.

THEORETICAL FORMULATION

The object of the algorithm is to compute the strain energy release rate $G(s)$ by equation (1). Consider the total potential functional,

$$\Pi = \int_\Omega \left(\int_0^{\varepsilon_{ij}} \sigma_{ij} \, \mathrm{d}\varepsilon_{ij} \right) \mathrm{d}\Omega + \int_\Omega f_i \cdot u_i \, \mathrm{d}\Omega + \int_{\partial\Omega} t_i \cdot n_i \, \mathrm{d}S \tag{2}$$

Without loss of generality we consider a linear elastic material for which the strain energy U is

$$U = \int_0^{\varepsilon_{ij}} \sigma_{ij} \, \mathrm{d}\varepsilon_{ij} = \frac{1}{2} \sigma_{ij}\varepsilon_{ij} \tag{3}$$

In the finite-element method the potential energy is approximated as

$$\Pi = \mathbf{u}^{\mathrm{T}} \left[\int_\Omega \frac{1}{2} \mathbf{B}^{\mathrm{T}} \mathbf{D} \mathbf{B} \, \mathrm{d}\Omega \right] \mathbf{u} + W \tag{4}$$

where $\mathbf{D}$ is the constitutive matrix, $\mathbf{B}$ is the strain-displacement matrix, W is the work performed by external loads, and $\mathbf{u}$ is the vector of nodal displacements.

The solution of the problem is obtained using the principle of virtual displacements (or the minimum total potential energy):

$$\frac{\partial\Pi}{\partial\mathbf{u}} = 0 \tag{5}$$

Since the approximate potential energy is a function of the nodal displacements $\mathbf{u}$ and the crack length $\mathbf{a}$, we have

$$\frac{\partial\Pi}{\partial a} = \frac{\partial\Pi}{\partial\mathring{a}} + \frac{\partial\mathbf{u}}{\partial a} \cdot \frac{\partial\Pi}{\partial\mathbf{u}} \bigg|_{a = \text{const}} \tag{6}$$

where

$$\frac{\partial}{\partial\mathring{a}} \equiv \frac{\partial}{\partial a} \bigg|_{\mathbf{u} = \text{const}} \tag{7}$$

Assuming that no body forces are present, no forces are applied to the surfaces of the crack, and the fixed-grip end condition (see appendix 6 of Reference 19 for an extended discussion) holds during the virtual crack extension, we obtain

$$\frac{\partial W}{\partial\mathring{a}} = 0 \tag{8}$$

and

$$\frac{\partial\Pi}{\partial\mathring{a}} = \frac{\partial U}{\partial\mathring{a}} = G \tag{9}$$

Using equations (5), (8) and (9) in equation (6), we obtain

$$\frac{\partial\Pi}{\partial a} = \frac{\partial\Pi}{\partial\mathring{a}} = \frac{\partial}{\partial\mathring{a}} \left\{ \mathbf{u}^{\mathrm{T}} \left[\int_\Omega \frac{1}{2} \mathbf{B}^{\mathrm{T}} \mathbf{D} \mathbf{B} \, \mathrm{d}\Omega \right] \mathbf{u} \right\}$$

or

$$G = \frac{\partial}{\partial\mathring{a}} \left\{ \sum_e \mathbf{u}^{\mathrm{T}} \left[\int_{\Omega_e} \frac{1}{2} \mathbf{B}^{\mathrm{T}} \mathbf{D} \mathbf{B} \, \mathrm{d}\Omega \right] \mathbf{u} \right\} \tag{10}$$

where Ω^e is a typical finite element. The indicated integration is carried out over the master element (see Reddy[18]):

$$G = \frac{\partial}{\partial q} \left\{ \sum_e \mathbf{u}^T \left[\int_{\Omega_e} \frac{1}{2} \mathbf{B}^T \mathbf{D} \mathbf{B} \, |J| \, d\xi \, d\eta \right] \mathbf{u} \right\} \tag{11}$$

Interchanging the order of integration and differentiation, which is possible because $\mathbf{u}$ is kept constant during the differentiation, we obtain

$$G = \frac{1}{2} \sum_e \mathbf{u}^T \left[\int_{\Omega_e} \frac{\partial}{\partial q} \left(\mathbf{B}^T \mathbf{D} \mathbf{B} \, |J| \, d\xi \, d\eta \right] \mathbf{u} \right\} \tag{12}$$

The integrand in equation (12) can be expanded as follows:

$$\frac{\partial}{\partial q} \left[\mathbf{B}^T \mathbf{D} \mathbf{B} \, |J| \right] = \frac{\partial}{\partial q} \left[\mathbf{B}^T \mathbf{D} \mathbf{B} \right] |J| + \left[\mathbf{B}^T \mathbf{D} \mathbf{B} \right] \frac{\partial |J|}{\partial q} \tag{13}$$

where

$$\frac{\partial}{\partial q} \left[\mathbf{B}^T \mathbf{D} \mathbf{B} \right] = \left[\frac{\partial \mathbf{B}}{\partial q} \right]^T \mathbf{D} \mathbf{B} + \mathbf{B}^T \mathbf{D} \left[\frac{\partial \mathbf{B}}{\partial q} \right]. \tag{14}$$

The strain displacement matrix $\mathbf{B}$ can be written in terms of the matrix of shape function Φ as

$$\mathbf{B} = \mathbf{J}^{-1} \Phi \tag{15}$$

and therefore

$$\frac{\partial \mathbf{B}}{\partial q} = \frac{\partial \mathbf{J}^{-1}}{\partial q} \Phi \tag{16}$$

Consider the identity

$$\mathbf{I} = \mathbf{J}^{-1} \mathbf{J} \tag{17}$$

Differentation with respect to a yields

$$0 = \frac{\partial \mathbf{J}^{-1}}{\partial q} \mathbf{J} + \mathbf{J}^{-1} \frac{\partial \mathbf{J}}{\partial q} \tag{18}$$

or

$$\frac{\partial \mathbf{J}^{-1}}{\partial q} = -\mathbf{J}^{-1} \frac{\partial \mathbf{J}}{\partial q} \mathbf{J}^{-1} \tag{19}$$

Substituting equation (19) in equation (16), we obtain

$$\frac{\partial \mathbf{B}}{\partial q} = -\mathbf{J}^{-1} \frac{\partial \mathbf{J}}{\partial q} \mathbf{J}^{-1} \Phi = -\mathbf{J}^{-1} \frac{\partial \mathbf{J}}{\partial q} \mathbf{B} \tag{20}$$

Equation (14) takes the form

$$\frac{\partial}{\partial q} \left[\mathbf{B}^T \mathbf{D} \mathbf{B} \right] = -\left[\mathbf{J}^{-1} \frac{\partial \mathbf{J}}{\partial q} \mathbf{B} \right]^T \mathbf{D} \mathbf{B} - \mathbf{B}^T \mathbf{D} \left[\mathbf{J}^{-1} \frac{\partial \mathbf{J}}{\partial q} \mathbf{B} \right] \tag{21}$$

Finally, combining equations (21) and (13), and inserting the result into equation (11), we

obtain the expression for the strain-energy release-rate,

$$G = \frac{1}{2} \sum_e \mathbf{u}^T \left[\int_{\Omega_e} \left\{ \left(-\dot{\mathbf{B}}^T \mathbf{D} \mathbf{B} - \mathbf{B}^T \mathbf{D} \dot{\mathbf{B}} \right) | J | + \mathbf{B}^T \mathbf{D} \mathbf{B} \frac{\partial | J |}{\partial q} \right\} \, dr \, ds \right] \mathbf{u} \tag{22}$$

where $\mathbf{u}$ is the displacement vector, known from the finite-element solution, and

$$\dot{\mathbf{B}} = \left[\mathbf{J}^{-1} \frac{\partial \mathbf{J}}{\partial q} \mathbf{B} \right] \tag{23}$$

The derivatives of the Jacobian must be computed as (note that $\partial \mathbf{J} / \partial q = \partial \mathbf{J} / \partial a$ since $\mathbf{J}$ is independent of $\mathbf{u}$)

$$\frac{\partial \mathbf{J}}{\partial q} = \begin{bmatrix} \sum_i \phi_{i,r} \dfrac{\partial x_i}{\partial q} ; & \sum_i \phi_{i,r} \dfrac{\partial y_i}{\partial q} ; & \sum_i \phi_{i,r} \dfrac{\partial z_i}{\partial q} \\[2ex] \sum_i \phi_{i,s} \dfrac{\partial x_i}{\partial q} ; & \sum_i \phi_{i,s} \dfrac{\partial y_i}{\partial q} ; & \sum_i \phi_{i,s} \dfrac{\partial z_i}{\partial q} \\[2ex] \sum_i \phi_{i,t} \dfrac{\partial x_i}{\partial q} ; & \sum_i \phi_{i,t} \dfrac{\partial y_i}{\partial q} ; & \sum_i \phi_{i,t} \dfrac{\partial z_i}{\partial q} \end{bmatrix} \tag{24}$$

where (r, s, t) are the local co-ordinates of the isoparametric element, (x_i, y_i, z_i) are the global co-ordinates of the nodes of the element and the vector

$$\mathbf{v} = \left\{ \frac{\partial x_i}{\partial q}, \frac{\partial y_i}{\partial q}, \frac{\partial z_i}{\partial q} \right\} \tag{25}$$

is the input vector that indicates the direction and shape of the virtual crack extension; $\partial | \mathbf{J} | / \partial q$ is evaluated similarly.[19] It is worth noting that the summation in equation (22) extends only over the elements connected to the crack because there is no deformation of the elements far away from the crack; that is, $\partial \mathbf{J} / \partial q = 0$ for elements not connected to the crack.

The evaluation of equation (22) requires the displacements $\mathbf{u}$ at the nodes of the (isoparametric) elements surrounding the crack. The elements used in the post-processor can be coded independently of those used in the finite-element program employed to obtain the displacements. At least in principle, they do not need to be of the same type. In this paper, however, both the main finite-element program and the post-processor use isoparametric quarter-point elements.

COMPUTATIONAL ASPECTS

In order to apply the method we must specify the direction of the virtual crack extension (but not its magnitude because it is a *virtual* crack extension). We give the direction of the VCE at least for each node on the crack front. However, for some meshes it is convenient to also use the mid-side nodes of the elements surrounding the crack front. Beyond that, any number of nodes can be used as long as they surround the crack front. The Jacobian derivative method uses the elements connected to these nodes to compute the strain energy release rate. Therefore the cost of the solution grows with the number of elements involved. But this cost is negligible compared to the cost of the finite-element analysis of the complete structure. Usually the solution is insensitive to the number of elements involved in the post-processing and only the crack tip elements need to be used.

All virtual crack extension methods rely on the displacement field obtained for the original crack shape. Therefore the virtual crack extension must be such that it preserves the shape of

the crack. If the shape of the crack were to change, the nature of the singularity would change significantly and the solution for the original shape would be of no help in predicting the new situation. For two-dimensional problems, this means that the direction of the VCE is that of the crack itself. For three-dimensional problems two aspects need to be considered. First, the VCE must lie on the plane of the crack. This is a natural extension of the two-dimensional argument. It does not mean that the crack cannot grow out of its plane. It just means that we are unable to compute anything else with just one solution for the original shape. Second, the VCE must have the shape of the original crack. Once again, it does not seem right to pretend to change the shape of the crack when we only have the solution for one shape. However, deviations to this premise have been reported in the literature with success. It is probable that no big errors are introduced violating the later requirement because the nature of the singularity supposedly does not change significantly as long as the crack remains in its original plane. The second requirement does not mean that the crack cannot grow with variable aspect ratio. Even more, we may be able to predict the direction of the growth based on the distribution of energy release rate along the crack front.

Since the Jacobian derivative method is a post-processor algorithm, we are tempted to use it with several probable shapes for the VCE. However, we have found that this is unnecessary. Just specifying a self-similar VCE we are able to compute the stress energy release rate distribution along the crack front of a curved crack. The Jacobian derivative method computes the contribution to the strain-energy release-rate $G(s)$ element by element. Computation of $G(s)$ along the crack front is explained in the three-dimensional applications presented in the following Section.

APPLICATIONS

In order to demonstrate the applicability of the proposed technique we present several numerical examples. Since it is computationally very expensive to use very refined meshes for three-dimensional problems we use coarse meshes in all the examples. We use collapsed, quarter-point elements around the crack tip[1-3] and quadratic isoparametric elements elsewhere.

Two-dimensional problems

We use a series of two-dimensional meshes with 17 quadratic elements and 62 nodes (see Figure 1) to study two problems:

(a) a plate with a single-edge crack
(b) a plate with a central crack.

The two cases differ only in the boundary conditions. In both cases, the load is uniform, applied as equivalent loads at the edge away from the crack. Symmetry along the crack line is exploited to model only one half of the specimen. We assume that a plane stress condition holds.

A three-dimensional analysis, performed for comparison, provides almost exactly the same result as the two-dimensional model.

The present finite-element solutions are compared with the solutions presented by Paris and Sih.[20] The results are tabulated in the form of correction factors to the stress intensity factor in an infinite medium k_0. Therefore the applicable stress intensity factor is $k = k_0 * f(a/b)$, with $k_0 = \sigma_0 (a\pi)^{1/2}$. Table I contains the results for a plate with a single-edge crack. The plate has
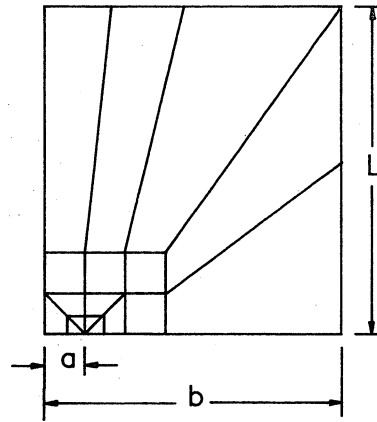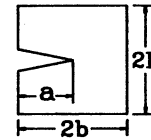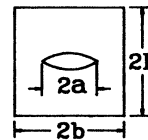
Figure 1. Two-dimensional finite-element mesh for plates with various through-the-thickness cracks

Table I. Values of $f(a/b)$ for a plate with single-edge crack

a/b	JDM	Gross	Bowie
0·2	1·19	1·19	1·20
0·4	1·38	1·37	1·37
0·6	1·86	1·66	1·68
0·8	2·14	2·12	2·14
1·0	2·83	2·82	2·86

Table II. Values of $f(a/b)$ for a plate with central crack

a/b	JDM $L/W = 1$	Hellen $L/W = 1$
0·1	1·02	1·02
0·2	1·06	1·05
0·3	1·13	1·12
0·4	1·23	1·21
0·5	1·34	1·33

length $2L$, width $2b = W$ and a crack of length a on one side. The finite-element solution is compared with the solutions presented in Reference 20. The agreement is excellent even for a coarse mesh. Table II contains the results for a square plate with at crack a the centre. The plate has length $2L$, width $2b = 2W$ and a crack of length $2a$. The present finite-element solution is compared with the solutions of Paris and Sih[20] for $L/W = \infty$ and the finite-element results of Hellen[4] for square plates. The agreement between the two finite-element solutions is excellent even for a coarse mesh.

Three-dimensional problems

Surface crack in a cylinder. Results are presented for a thick cylinder of internal radius
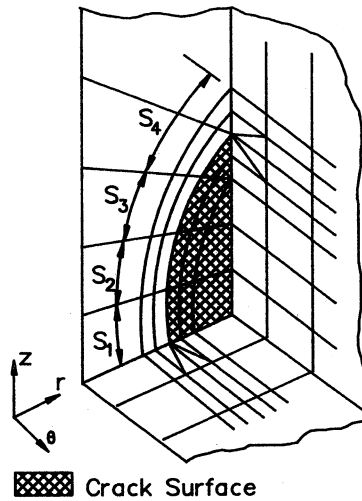
Figure 2. Detail of the cracked area of the cylinder with external crack. Only part of the mesh is shown. Hidden lines have been removed

$R_i = 29.8$ mm, thickness $t = 5$ mm, length $2b = 200$ mm, subjected to internal pressure P. A surface crack is located longitudinally on the outer surface. The shape of the crack is that of a segment of a circle (see insert in Figure 3 with $a = 2.3$ mm, $1c = 13.6$ mm. Kaufmann et al.[21] presented experimental and numerical results for this particular crack shape.

A mesh with 275 elements and 4107 degrees of freedom is used to obtain the displacement field around the crack front. A layer of 22 collapsed, quarter-point elements[1,2] surround the crack front. Quadratic isoparametric elements model the rest of the specimen. Detail of the mesh around the crack front is shown in Figure 2. Four segments labelled S_1 to S_4 divide one half of the crack front. On each segment, four collapsed elements surround the crack front. The mesh becomes coarse rapidly toward the main portion of the cylinder.

The virtual crack extension direction is specified so as to produce a self-similar growth of the crack. All the nodes of the elements surrounding the crack front are used in the VCE. These elements are those in the inner layer next to the crack front (see Figure 2). Therefore, for this example, the algorithm uses the two layers of elements surrounding the crack front to compute the strain energy release rate.

The Jacobian derivative method computes the contribution to the strain-energy release rate element by element. Next, we add the contributions to the strain energy release rate of all the elements that surround one sector (S_i) of the crack front at a time (see Figure 2).

Then we divide this value by the length of the crack front covered by the corresponding sector (S_i) to obtain the distribution of the strain energy release rate along the crack front.

In order to compare the results with others, we transform $G(s)$ to $K(s)$ by means of either a plane strain or plane stress assumption, whichever is appropriate:

$$\text{plane stress: } K(s) = \sqrt{\{EG(s)\}}$$

$$\text{plane strain: } K(s) = \sqrt{\left\{\frac{EG(s)}{1 - \nu^2}\right\}}$$

The distribution of $K(s)$ is shown in Figure 3 for the plane strain assumption, along with results from Kaufman et al.[21] The results are normalized by the stress intensity factor K_0 at

$\phi = \pi/2$ for an elliptical crack embedded in an infinite body subjected to a uniform stress

$$K_0 = \frac{2R_i^2 P}{R_0^2 - R_i^2} \sqrt{\left\{ \frac{\pi a}{1 + 1 \cdot 464 \, (a/c)^{1 \cdot 65}} \right\}}$$

Kaufman *et al.*[21] computed the stress intensity factor using the plane strain assumption and the method of Reference 7. In our case, the distribution of $G(s)$ is obtained directly from the three-dimensional analysis without any two-dimensional assumption. The solution by the present method closely agrees with that presented in Reference 21.

Side-grooved compact test specimens. It is well known that the compact test specimen shows a small variation of the stress intensity factor along the crack front.[22,23] However, if the sides of the crack are grooved (see Figure 4) the stress intensity factor has an important variation through the thickness. Reference 24 presents numerical results and experimental evidence that the stress intensity factor grows considerably at the grooved side.

The geometry of the specimen is shown in Figure 4. Owing to symmetry only a quarter of the specimen is modelled. A finite-element mesh of 370 quadratic elements with 1985 nodes is uniformly refined toward the side of the specimen and toward the crack front. 3-D collapsed, quarter-point elements surround the crack front. Only elements surrounding the crack front
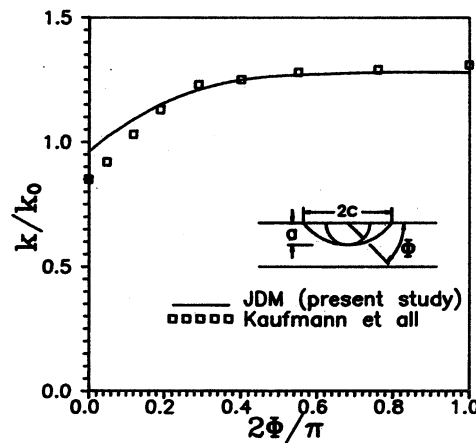

Figure 3. Stress intensity factor distributions along the crack front of an external surface crack on a cylinder under internal pressure
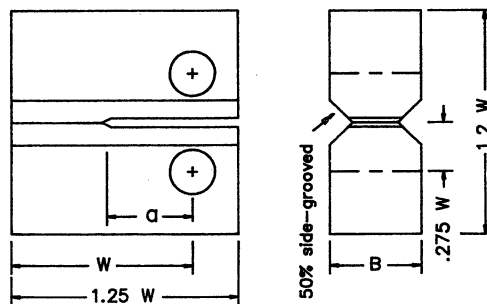

Figure 4. Side and front view of the 50% side-grooved compact-test specimen; $B = 0 \cdot 5 \, W$, $a = 0 \cdot 6 \, W$
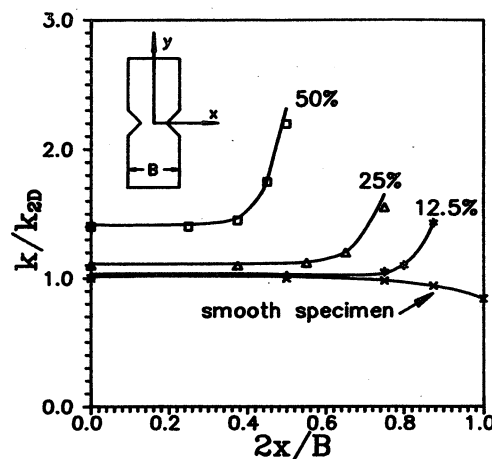
Figure 5. Through-the-thickness distribution of the stress intensity factor normalized with respect to the boundary collocation solution[25] for the smooth specimen x, 12·5% slide-grooved ★, 25% side-grooved Δ and 50% side-grooved □. Solid lines from JDM and symbol markers from Reference 24

are used in post-computation by the JDM. The plane-strain equations are used to transform the strain energy distribution along the crack front to a stress intensity factor distribution. The results are normalized with respect to the 2-D boundary collocation solution.[25]

The thickness distribution of the stress intensity factor along the crack front for compact test specimens with and without grooved sides are shown in Figure 5 for $a = 0·6\ W$ and $B = 0·5\ W$. The solid lines represent the results of the present study (JDM) and symbol markers are taken from Figure 4 of Reference 24. The maximum value for the smooth specimen differs by less than 0·2% from the value reported in Reference 24 for $a = 0·5\ W$. The agreement is excellent, except perhaps for the 50% side-grooved specimen, where differences in the finite-element mesh and in the Poisson ratio may have more influence than in the other cases. Although the Poisson ratio was not reported in Reference 24 its effect on the stress intensity factor is small, at least for the two-dimensional problem[25]. In this study we used: $\nu = 0·33$ and $E = 10^7$. This example further demonstrates the applicability of the JDM to accurately evaluate the stress intensity factor distribution along the crack front of 3-D fractures.

CONCLUSIONS

A novel method of computing energy release rates and stress intensity factors is described and its application to 2-D and 3-D problems is illustrated via specific examples. The Jacobian derivative method (JDM) developed herein keeps all the advantages of the indirect methods while adding new enhancements. Being an indirect method, it can be used with displacements obtained with a variety of techniques. In particular, even experimental techniques can be used. The method does not require costly mesh refinements, and it is not mesh-sensitive. Unlike the VCEM, it does not require the specification of a small crack extension, which makes the JDM a more robust algorithm. Its applicability for three-dimensional curved cracks is demonstrated. Application to delaminations in composite materials along with refined plate theories is reported in Reference 19.

REFERENCES

1. R. D. Henshell and K. G. Shaw, 'Crack tip elements are unnecessary', *Int. j. numer. mehods eng.*, **9**, 495–507 (1975).
2. R. S. Barsoum, 'Application of quadratic isoparametric finite elements in linear elastic fracture mechanics', *Int. J. Fract.*, **10**, 603–605 (1975).
3. R. S. Barsoum, 'Triangular quarter point elements as elastic and perfectly-plastic crack tip elements', *Int. j. numer. methods eng.*, **11**, 85–98 (1977).
4. T. K. Hellen, 'On the method of virtual crack extensions', *Int. j. numer. methods eng.*, **9**, 187–207 (1975).
5. D. M. Parks, 'A stiffness derivative finite element technique for determination of elastic crack tip stress intensity factors', *Int. J. Fract.*, **10**, 487–502 (1974)
6. P. Tong, T. H. H. Pian and S. J. Lasry, 'A hybrid-element approach to crack problems in plane elasticity, '*Int. j. numer. methods Eng.*, **7**, 297–308 (1973).
7. S. K. Chan, I. S. Tuba and W. K. Wilson, 'On the finite element method in linear fracture mechanics', *Eng. Fract. Mech.*, **2**, 1–17 (1970).
8. I. S. Raju and J. C. Newman, 'Three-dimensional finite element analysis of finite-thickness fracture specimens', NASA TN D-8414, 1977.
9. I. S. Raju and J. C. Newman, 'Stress-intensity factors for a wide range of semi-elliptical surface cracks in finite-thickness plates', *Eng. Fract. Mech.*, **11**, 817–829 (1979).
10. J. R. Rice, 'A path independent integral and the approximate analysis of strain concentrations by notches and cracks', *J. Appl. Mech.*, **35**, 379–386 (1968).
11. E. F. Rybicki and M. F. Kanninen, 'A finite element calculation of stress intensity factors by a modified crack closure integral', *Eng. Fract. Mech.*, **9**, 931–938 (1977).
12. T. S. Ramamurthy, K. Krishnamurthy, and K. Badari Narayana, 'Modified crack closure integral with quarter points elements', *Mech. Res. Commun.*, **13** (4), 179–186 (1986).
13. J. L. Coulomb, 'A methodology for the determination of global electromagnetical quantities from a finite element analysis and its application to the evaluation of magnetic forces, torques and stiffness, '*IEEE Trans.*, **MAG-19**(6), 1983.
14. K. J. Bathe and T. D. Sussman, 'An algorithm for the construction of optimal finite element meshes in linear elasticity', *Computer Methods for Nonlinear Solids and Structural Mechanics*, **AMD-54**, 15–36 (1983).
15. R. B. Haber and H. M. Koh, 'Explicit expressions for energy release rates using virtual crack extensions', *Int. j. numer. methods eng.*, **21**, 301–315 (1985).
16. H. G. DeLorenzi, 'Energy release rate calculations by the finite element method', *Eng. Fract. Mech.*, **21**(1), 129–143 (1985).
17. S. C. Lin and J. F. Abel, 'Variational approach for a new direct-integration form of the virtual crack extension method, *Int. J. Fract.*, **38**, 217–235 (1988).
18. J. N. Reddy, *An Introduction to the Finite Element Method*, McGraw-Hill, New York, 1984.
19. E. J. Barbero, 'On a generalized laminate theory with application to bending vibration, and delamination buckling in composite laminates' Ph.D. Dissertation, Virginia Polytechnic Institute and State University, October 1989.
20. P. C. Paris and G. Sih, 'Fracture toughness testing and its applications', *ASTM Special Technical Publication*, No. 381, 30–81, 1965.
21. G. H. Kaufmann, A. M. Lopergolo, S. R. Idelsohn and E. J. Barbero, 'Evaluation of finite element calculations in a part-circular crack by coherent optics techniques', *Experimental Mechanics*, 154–157 (1987).
22. I. S. Raju and J. C. Newman, Jr., 'Methods for analysis of cracks in three-dimensional solids', NASA Technical Memorandum 86266, July 1984.

23. A. A. Tseng, 'A comparison of finite element solutions for the compact specimen', *Int. J. Fract.*, **17**, 125–129 (1981).
24. C. F. Shih and H. G. deLorenzi, 'Elastic compliances and stress-intensity factors for side-grooved compact specimens', *Int. J. Fract.*, **13**, 544–548 (1977).
25. J. C. Newman, Jr, 'Stress analysis of the compact specimen including the effects of pin loading', *Fract. Anal.*, ASTM STP, **560**, 105–121 (1973).